Desalination and Water Treatment
www.deswater.com

doi: 10.1080/19443994.2014.980333

56 (2015) 3476–3485
December

Taylor & Francis
Taylor & Francis Group

Iron influence on uranium removal from water using cellulose acetate membranes doped with activated carbon

R. Villalobos-Rodríguez[a], K. Ruíz Cuilty[a], M.E. Montero-Cabrera[a,*], H.E. Esparza-Ponce[a], G.V. Nevarez-Moorillon[b], V. Fierro[c], A. Celzard[c], M.L. Ballinas-Casarrubias[b]

[a]*Centro de Investigación de Materiales Avanzados (CIMAV). Miguel de Cervantes 120 Compl. Ind. Chihuahua, CP 31109 Chihuahua, Chih., Mexico, Tel. +52 614 4391100; emails: ruben.villalobos@cimav.edu.mx (R. Villalobos-Rodríguez), karla.ruiz@cimav.edu.mx (K. Ruíz Cuilty), elena.montero@cimav.edu.mx (M.E. Montero-Cabrera), hilda.esparza@cimav.edu.mx (H.E. Esparza-Ponce)*
[b]*Facultad de Ciencias Químicas, Universidad Autónoma de Chihuahua, Nuevo Campus s/n, Chihuahua, Chih, Mexico, Tel. +52 614 2366000; emails: vnevare@uach.mx (G.V. Nevarez-Moorillon), mballinas@uach.mx (M.L. Ballinas-Casarrubias)*
[c]*Institut Jean Lamour—UMR CNRS 7198, University of Lorraine, ENSTIB, 27 rue Philippe Séguin, CS 60036, 88026 Epinal Cedex, France, Tel. +33 329296100; emails: vanessa.fierro@univ-lorraine.fr (V. Fierro), alain.celzard@univ-lorraine.fr (A. Celzard)*

Received 14 July 2014; Accepted 10 October 2014

ABSTRACT

Ultrafiltration removal of uranium from water was investigated using cellulose triacetate–activated carbon (CTA–AC) composite membranes. Two different approaches were adopted: (i) adding iron chloride to the uranyl solution ($FeCl_3$ at 0.5, 1.0, and 2.0 ppm), and (ii) filtration of pure uranyl nitrate throughout composite membranes made of CTA filled with AC doped with iron. The solution to be filtrated was mixed with uranyl nitrate dissolutions at very low concentration (1.2 ppm), with pH 6–8. AC was added to CTA using a casting film process to obtain dense membranes. Average uranium removal was 22 ± 3%. The presence of iron in the membrane, either dissolved or incorporated into the activated carbon, contributed to uranium filtration, allowing reaching up to 50% removal efficiency (RE). The lowest RE value (4%) was obtained using a membrane prepared with AC oxidized with nitric acid (3HNO-AC) which does not present a significant amount of iron. Another parameter driving uranium transport is the pH, as uranium forms high molecular weight compounds in alkaline solutions, and therefore remains trapped into membrane structure. This explains the RE value of 21%, using 3HNO-AC membrane at high pH. AC dispersion also plays an important role during uranium transport. If it is well dispersed into the polymeric matrix, high RE is attained due to the high surface area available into the material. On the contrary, if AC agglomerates, uranium can go throughout the membrane, thereby increasing its permeability.

Keywords: Uranium in solution; Ultrafiltration by membranes; Iron influence

---

*Corresponding author.

Presented at the IX Ibero-American Congress on Membrane Science and Technology (CITEM 2014), 25–28 May 2014, Santander, Spain

1. Introduction

Uranium pollution in water is an issue of global concern, mainly due to water scarcity for human consumption worldwide. This actinide has been gradually introduced into ground water through mining and as a naturally-leaking mineral. Uranium has toxic effects mainly in the urinary system. Another related health risk is that uranium is converted into other highly toxic radioactive species, which can cause cancer. Thus, based on a wide variety of studies, USEPA has set a maximum acceptable uranium level of 30 μg L^{-1} and 15 pCi L^{-1} (0.56 Bq L^{-1}) for alpha particles [1].

In Mexico, NOM-127-SSA1–1994 establishes the highest limit for global alpha radioactivity at 0.56 Bq L^{-1} [2]. Particularly, uranium pollution in water has been widely studied in the north part of the country [3,4]. Its concentration ranges from 0.03 to 1.34 Bq L^{-1}. These levels are reached due to natural lixiviation mechanisms. For example, some of the minerals identified in the San Marcos region, which provides water to Sacramento River located near Chihuahua City, are uraninite, pechblende, uranophene, tyuyamunite, and becquerilite [4]. Therefore, affordable separation techniques are necessary to diminish health risks by eliminating or reducing uranium presence from surface and groundwater sources. Considering this situation, several osmosis plants for water purifications had been established throughout Chihuahua State. Nevertheless, this technology is time and cost consuming, due to high energy requirements and membrane replacement costs necessary for maintenance. Thus, it is desirable to develop cost-effective materials to improve water quality for consumption.

Some of the adsorbents reported for uranium removal from water are hydroxyapatite [5,6], with efficiencies higher than 80%; chitosan [7] used for high uranium concentration (90 mg L^{-1}); activated carbon [8–10], carbon nanotubes [11], zero-valent iron [12–14], and iron oxides [15–18]. The latter can reach uranium removal efficiencies higher than 90%. Other methods reported so far are: coagulation–flocculation [19,20] and ion exchange resins [21,22]. All these methods present high uranium removal efficiencies, but, to work properly, also require high uranium concentration, large contact time and acidic pH. These conditions are not representative of the parameters found in ground water, where basic pH and low uranium concentration prevail.

Some works have explored the use of extractants in the membrane to favor the removal efficiency (RE) of radioactive species. The extractants used for uranium are more often di-(2-ethylhexyl) phosphoric acid (HDEHP) and tri-octyl-phosphine oxide, although Alamine 336, Cyanex 272 and aliquat 336 [23–26] have also been used. The literature reports other extractants for metal ions, such as tri-butyl phosphate, crown ethers or solutions of quaternary and tertiary amines, which also have been used in the extraction of uranium for analytical purposes [27–32].

Because of the aforementioned conditions, membrane technology is the most suitable technology for uranium removal [33]. For instance, nanofiltration removes more than 70% of uranium from water [34,35], and uranium ultrafiltration with a previous complexation reaction using polyethylenimide [36] and using aromatic polyamide membranes [37] have been reported. These processes are cheaper than reverse osmosis, especially due to the lower operating pressures required.

In this regard, a former work has been carried out to develop an ultrafiltration membrane to be used for uranium removal [38]. Scientific literature does not report uranium removal, from environmental concentration solutions, through cellulose triacetate (CTA) membranes. Cellulose can be obtained from agro-industrial activities wastes, and its use may favor a sustainable development. In the present work, based on the activated carbon capacity for uranium retention, a composite membrane with CTA has been developed and tested in absence or presence of trivalent iron in synthetic water. Besides, iron-loaded activated carbon has been used as filler of composite membranes, and its effect is studied in membrane permeation processes.

2. Materials and methods

2.1. Characterization and synthesis

Filtration experiments were carried out in two parts. In the first part, a uranyl nitrate solution was used with a cellulose triacetate—iron-loaded activated carbon composite membrane (CTA–FeAC). In the second part, a synthetic uranyl nitrate—ferric chloride solution was used with a cellulose triacetate—activated carbon composite membrane (CTA–AC) for uranium permeation testing.

2.1.1. Activated carbon pretreatment

Details of this activated carbon pretreatment were reported previously by Muñiz et al. [39–41]. For the first part of the experiments, activated carbon NC-100 (Norit) previously doped with iron was used for composite preparation. The NC-100 carbon was immersed in nitric acid at 80˚C, and stirred for 3 h to obtain an oxidized carbon labelled 3HNO. This carbon was next impregnated during different times with $FeCl_3$ dissolved in HCl: 3, 6 and 24 h [39,40], and the resultant materials were labelled Fe3H, Fe6H and Fe24H, respectively. Lactones, carbonyls and phenolic groups have been already evidenced in 3HNO carbon, with a total of 1.5 meq/g acid groups and 0.72 meq/g of basic ones, giving up a final pH of 4.8 [41].

AC doped with iron by exhaustive hydrolysis evidenced oxi-hydroxide iron nanoparticles finely distributed on the carbon surface. The maximum iron agglomeration occurred for after 24 h of treatment with iron chloride. Iron content was analyzed for the three carbons. Thus, 2, 2.2, and 9.4% of iron were found for 3, 6, and 24 h of hydrolysis, respectively.

In the second part of experiments, composite membranes with LQ1000 (Carbochem) carbon were obtained. For LQ1000 AC, Al, Ca and Si were found, as it was previously reported [42]. These features evidence the presence of ashes into the carbon.

For composite production in both parts, carbon was milled (Spex 8000D Mixer/mill). For non—iron-loaded AC, a solvation pretreatment using THF was followed as reported elsewhere [43].

2.1.2. Membrane synthesis

Membranes were obtained by an evaporation–precipitation method using a humidity-temperature controlled chamber (SHEL LAB /HC5). Membranes were prepared at 45 ℃ and 70% relative humidity. Membranes were obtained by dissolving 5 g of CTA (Aldrich) in 200 mL of methylene chloride (CH_2Cl_2, J.T. Baker). A suspension of AC (0.05 g in 50 mL of CH_2Cl_2) was used to prepare 1% AC composites. The solution and the suspension were stirred for 24 h separately. Afterwards, they were blended, and stirring continued for 24 additional hours. The final mix was processed in a sonicator (Karl Roll-RSW) for 3 h, maintaining the mixture volume. Finally, 25 mL of the solution were poured into a 9.5 cm petri dish and evaporated for 90 min.

2.1.3. Scanning electronic microscopy–energy dispersive spectrometry

The composition of activated carbons used in the membranes was analyzed by scanning electron microscopy (SEM) JSM-5800LV coupled with energy dispersive spectrometry (EDS) analyzer (EDAX DXprime model). The morphology and composition of CTA–AC, before and after filtration were evaluated. Carbons samples were analyzed as such, but the membranes were metallized by sputtering a gold thin film (10 nm) in a Denton Vacuum Desk IV prior to SEM observation. Carbons and membranes were observed at 15 kV and 0˚ tilt at different magnifications. EDS X-ray analysis gives information about elemental mass and/or atomic percentage. The analyzed depth depends on voltage, and was almost 100 nm in the present case. The software used for elemental analyses was EDX-ZAF.

2.1.4. Atomic force microscopy

Membrane surface roughness (Rms) was measured by tapping-AFM (Multimode AFM Nanoscope IVa) in an intermittent mode. Samples were placed onto stainless steel discs with an adhesive tape. The tip used was in silicon, 225 μm length (TESP Veeco) and presented an optimal frequency range between 272 and 334 kHz. The scan rate was 1 Hz. Image analysis was made using WSxM 3.0 software [44]. The average and standard deviations (SD) of obtained roughness values were calculated using the data at five points for each membrane.

2.2. Membrane permeation

Filtration experiments were made using a filtration cell, constructed in scale of SEPA CF II from GE Osmonics [38]. For each experiment, 2.6 L of uranyl nitrate were filtered tangentially, and pumped by a peristaltic pump. Details of experimental procedure were described elsewhere [38].

2.2.1. Uranyl nitrate solutions

Two uranyl nitrate (SPI-CHEM) stock solutions were prepared for the filtration experiments described below.

The first part of the experiments were done using CTA–FeAC membranes with stock solution #1, that was prepared by dissolving 0.533 g of uranyl nitrate (equivalent to 0.253 g of uranium) into 250 mL tri distilled water (HIDROGEL brand). The pH of the three aliquots used was adjusted at 6.0, 7.0, and 8.0. Aliquots were made by diluting 3 mL of the stock solution #1 into 3 L of distilled water (J.T. Baker).

In the second part of filtrations, CTA–AC membranes were used, and stock solution #2 was employed. To prepare this solution, 0.632 g of uranyl nitrate (equivalent to 0.30 g of uranium) were dissolved in 250 mL of tri distilled water to make a 1,200 ppm uranium solution. The pH was fixed at 8.0, using HCl and/or NaOH. Three aliquots were prepared by diluting 3 mL of the stock solution #2 into 3

L of distilled water. To this set of solutions, iron was added in the form of iron chloride, to achieve 0.5, 1.0, and 2.0 ppm of iron. Iron was finally quantified by ICP (ICP-MS: Thermo Electron X Series II).

Table 1 provides a summary of the experimental conditions employed in the present work.

2.2.2. Uranium RE

The radioactivity concentration of input, permeated and rejected solutions were determined using a liquid scintillation counter (LSC Triahler Hidex type 425-034) by the external standard relative method [45,46]. For solutions of type #1, i.e. containing uranyl nitrate alone, aliquots of 4 mL were acidified with nitric acid to pH ≤ 2 and added to 16 mL of the liquid scintillator Ultima Gold AB (PerkinElmer). The detection efficiency for type #1 solutions was 0.967 ± 0.004. For solutions of type #2, i.e. which also contained $FeCl_3$, nitric acid was added to 400 mL aliquots to obtain pH ≤ 2. This liquid was evaporated to 200 mL and then 2 mL of HDEHP (Alfa Aesar) was added for uranium extraction. The solution was stirred and then stood until phase separation. The aqueous phase was discarded and the organic phase was added to 18 mL of Ultima Gold AB. In this case, the detection efficiency was 0.796 ± 0.003. The same procedures were applied to determine the background for each type of experiment, applying them to 4 and 400 mL of distilled water, respectively. The reference for relative analysis was obtained from a uranyl nitrate solution (High Purity Standards 100064), with a certified concentration of 1,000 ± 3 mg mL^{-1}. Consequently, 165 μL and 0.2 mL of uranium standard were added to 3.835 mL and 400 mL of distilled water, respectively and the corresponding procedure was performed to determine their activity. Associated uncertainties were also determined when applying all procedures. More details of these procedures were given elsewhere [38].

Table 1
Iron content and characteristics of the synthetic solutions for each membrane type employed in the experiments

Membrane type	Fe content	Aqueous solution employed
3HNO	840 ppm	Uranyl nitrate stock solution #1, with 1,010 ppm of U
Fe3H	2%	Solutions with 1 ml of the stock uranyl solution #1 diluted in 1 L distilled water; pH 6, 7, and 8
Fe6H	2.2%	
Fe24H	9.4%	
LQ 1000	none	Uranyl nitrate stock solution #2, with 1,200 ppm of U Three solutions of 1 ml of the stock uranyl solution #2 diluted in 1 L distilled water, added with ferric chloride to get iron concentrations of 0.5, 1.0, and 2.0 ppm, respectively; pH 8

Calculation of relative filtration and removal efficiencies was done using the results of the activity concentrations determined as described above and applying the following expressions:

$$FE = \frac{\text{A filtration}}{\text{A input}} \tag{1}$$

$$RE = 1 - FE \tag{2}$$

where FE = Filtration efficiency, RE = Removal efficiency, A filtration = Activity concentration of filtered solution, A input = Activity concentration of input solution

2.2.3. Speciation analysis

Chemical theoretical speciation was calculated using HYDRA/MEDUSA software (42 bit, Version 26 August 2009) [47].

2.2.4. Statistical analysis

For membrane roughness analysis obtained by AFM, a one-way analysis of variance was used to determine differences among the membranes utilized. For uranium removal efficiencies obtained in Experiment 1, the data were analyzed by ANOVA for factorial design, using pH and membrane composition as independent variables; Tukey analysis of means was further used when a statistical significance was found ($p < 0.05$). The statistics software used was MINITAB version 17.

3. Results

3.1. SEM–EDX

In the first part of the study, AC doped with iron was used for composite membrane production. In this study, EDS was used for AC characterization. In all doped AC, the following elements were detected: Fe, C, O, and Cl. For the second part of experiments, AC without iron was used for composite membranes.

SEM images were obtained for composite membranes made with 3HNO, Fe3H, Fe6H, Fe24H and LQ1000 AC, with a magnification of 450× (Fig. 1).

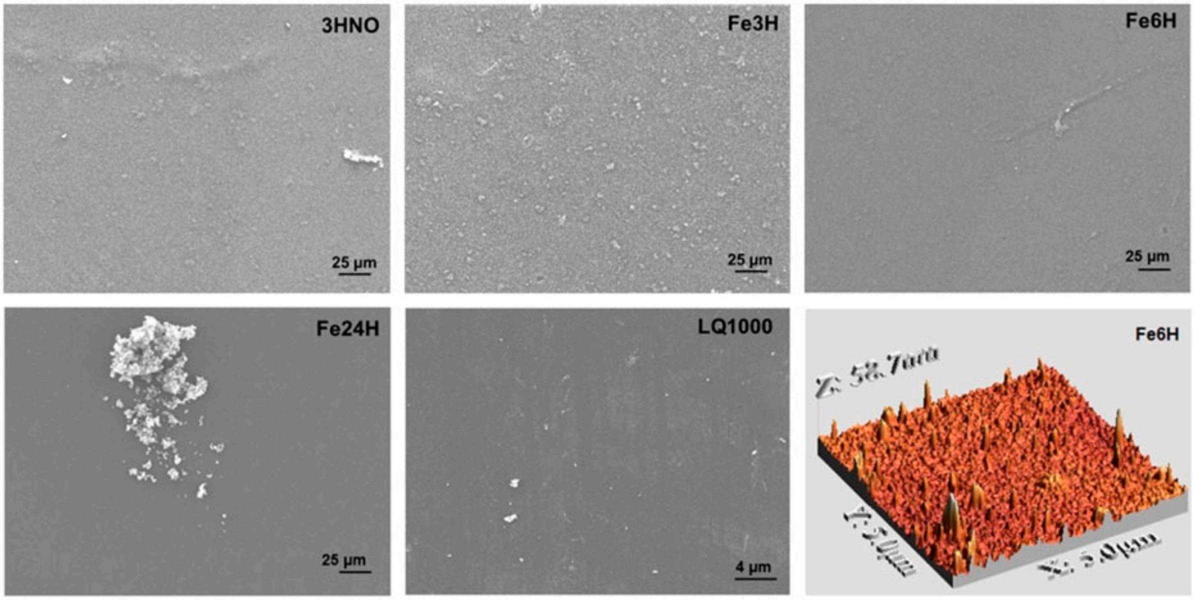

Fig. 1. SEM micrographs of all membranes at magnification 450×. Identification is shown in the upper right corner. A topographic AFM image of the membrane based on Fe6H is added for better roughness assessment.

SEM images show evidence of carbon agglomeration for almost all membranes tested. The best AC distribution was obtained in the CTA–Fe6H-AC membrane. EDS analysis revealed C, O, Si, Al, Ca, Na, and Cl for 3HNO-based membrane; C, O, Cl, Ca, and Fe in the Fe3H-based one; and C, O, Ca, Si, Al, Cr, V, and Fe in the Fe6H-based membrane. The behavior of iron in membranes may be explained by the nature of the activated carbon employed in membrane synthesis. Ferric chloride forced hydrolysis is a good method for increasing the iron content of activated carbons. Activated carbons with iron contents ranging from 1.5 to 9.4% were obtained [40,41]. The amount of deposited iron increased linearly with hydrolysis time. Iron-based nanoparticles, extremely small, homogeneous in size, and well-dispersed in the carbon matrix, were obtained. However, nanoparticles forming clusters over the outer surface of the carbon grains at hydrolysis times higher than 6 h were also produced. Agglomerates with a size ranging from 50 to 100 nm and composed of iron (hydr)oxide nanoparticles were found in the AC prepared by forced hydrolysis during 24 h.

3.2. *Atomic force microscopy*

Atomic force microscopy (AFM) analysis was done for the same membranes as those studied by SEM. Table 2 gathers the roughness values of the membranes, which were calculated considering four different regions of each membrane material. It is important to consider that roughness affects membrane flux processes.

As it can be observed, Fe6H-based composite is the smoothest membrane, even considering the large scattering of roughness measurements. Statistical analysis on the roughness among all membranes (One-way ANOVA, $p > 0.05$) showed that there were no statistical differences among them. This statistical result is obtained due to the procedure applied for quantification of the roughness (see Section 2.1.4) by measuring the Rms deviation of the surface level at 5 points of the membrane, and then calculating the SD between the direct measurements. If the membranes are not homogeneous, the SD will be large and the ANOVA will report that the differences between the membranes, as a whole, are not significant. A topographic AFM image of membranes produced using WSxM software for image analysis was also done, and the image for the Fe6H-based membrane is included in Fig. 1. In nanofiltration

Table 2
Roughness values of the membranes, measured by AFM

Membrane	Roughness (nm)
3HNO	21.06 ± 12.16
Fe3H	44.64 ± 25.78
Fe6H	16.07 ± 9.28
Fe24H	17.39 ± 10.04
LQ1000	16.34 ± 9.43

membranes, a low roughness value is desirable since lower roughness leads to lower membrane fouling during the separation process [48].

3.3. Membrane permeation

For membrane filtrations, two different experiments were performed. The first one was done using composites with iron-loaded activated carbon and uranyl nitrate solutions. The second one was carried out using composites with LQ1000 AC. In this second set of experiments, iron concentration in solution was varied from 0 to 2 ppm, using $FeCl_3$ (see Section 2.2.1).

3.3.1. Uranyl filtration by iron-loaded AC composites

Uranium rejection (see Section 2.2.2) was calculated and the corresponding results are shown in Table 3. Flux average value was 48.86 L bar^{-1} m^{-2} h^{-1}, at a pressure of 9.13 bar, thus corresponding to a nanofiltration process.

The data were analyzed by factorial ANOVA, to determine the effect of pH, iron content in the membrane and the interaction of those factors, on the removal efficiencies. According to the results, the iron content resulting from the membrane and the treatment used, the pH of the filtrated solution, as well as the interaction of both factors, showed statistical significance ($p < 0.001$). The membrane based on 3HNO was different from those made with FeAC, the latter not showing differences of uranium RE (Tukey analysis of means, $p < 0.05$). The pH had a highly significant effect on uranium removal, and the best results among all membranes was obtained at pH 8.0 (ANOVA $p < 0.001$; Tukey analysis of means $p < 0.05$).

Membrane performance was affected by the pH of the uranium solution, as confirmed by the statistical analysis. It shows highly significant interaction between the two factors was found ($p < 0.001$). The best results were obtained with the Fe6H-based membrane in slightly basic media (pH 8.0). For membrane with the maximum iron concentration in the AC, the lowest pH was the best for uranium rejection. A summary of the statistical analysis results, provided by the equation of the response surface and the corresponding graphical information, is shown in Appendix A.

Table 3
Removal efficiencies of different CTA–FeAC membranes at three pH. Two independent replicates are shown. SDs are calculated based on 3 radioactivity measurements

Sample	pH 6.0	pH 7.0	pH 8.0
3HNO	0.04 ± 0.01	0.10 ± 0.02	0.21 ± 0.04
	0.12 ± 0.02	0.08 ± 0.02	0.19 ± 0.03
Fe3H	0.30 ± 0.04	0.18 ± 0.03	0.20 ± 0.03
	0.36 ± 0.05	0.16 ± 0.02	0.23 ± 0.04
Fe6H	0.17 ± 0.03	0.18 ± 0.03	0.50 ± 0.07
	0.18 ± 0.04	0.16 ± 0.03	0.44 ± 0.06
Fe24H	0.39 ± 0.06	0.29 ± 0.05	0.15 ± 0.03
	0.36 ± 0.06	0.26 ± 0.04	0.16 ± 0.03

When the iron is well dispersed into AC, and when the carbon is evenly distributed in the composite, the higher rejection is attained for basic pH. Taking into account the previously reported results [39], iron in carbon forms oxi-hydroxides which might be the main reason of uranium adsorption. As suggested before [38], uranium might develop complexes in the form of carbonate species with iron in the form of Fe(III) [49,50]. These compounds have been extensively reported as adsorbents for uranium, e.g. iron oxides [51,52], bacterial iron oxides [18], hematite [17] and magnetite [53].

In the case of Fe24H-based membranes, iron is agglomerated at the AC surface [39]. This situation probably leads the rejection process because iron effective surface concentration might be lower than in Fe6H-based membranes, as it was evidenced by SEM–EDS (view Section 3.1). As iron is not effectively

Table 4
Rejection efficiencies for membranes with LQ1000 AC at different iron concentrations in the solution. SDs are calculated based on 3 radioactivity measurements

pH 8.0	0.5 ppm Fe	1.0 ppm Fe	2.0 ppm Fe
LQ1000	0.08 ± 0.01	0.34 ± 0.04	0.20 ± 0.03
	0.12 ± 0.01	0.36 ± 0.04	0.25 ± 0.04

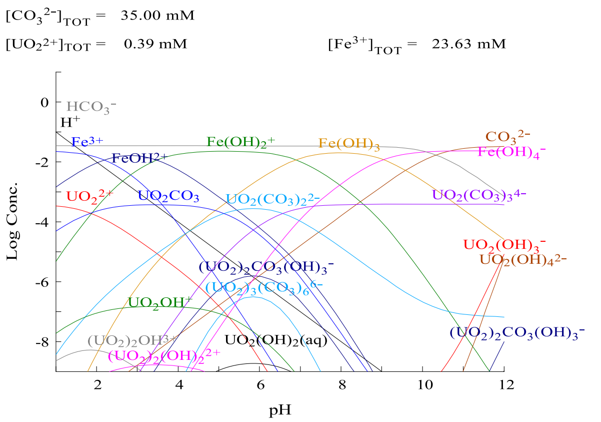

Fig. 2. Speciation diagram for uranium and iron in solution at different pH. Ion concentrations used in the calculations are given above the diagram.

Table 5
Long-time filtration of a solution containing 1,200 ppm of uranium and 2 ppm of iron. SDs are calculated based on 3 radioactivity measurements

Filtration	Time (h)	Volume (L)	Pressure (bar)	Flux ($Lm^{-2}\ bar^{-1}\ h^{-1}$)	RE
1	36.6	33.8	10.01 ± 1.39	79.85	0.26 ± 0.04
2	31.3	31.2	9.81 ± 1.75	87.98	0.18 ± 0.03

interacting with uranium carbonate species, basic media does not favor uranium rejection.

3.3.2. *Uranyl + $FeCl_3$ solution filtration by LQ1000 AC composites*

In the second part of the experiments, rejection was calculated for membrane filtrations at different iron concentrations. In this case, the pH was fixed at 8, in agreement with previously reported data [38]. The results are presented in Table 4. Maximum uranium rejection was now attained at 1.0 ppm of iron in the form of Fe(III) in solution. Average flux for all these filtrations was 89.03 $L\ bar^{-1}\ m^{-2}\ h^{-1}$, at 8.52 bar of pressure, thus a nanofiltration process was achieved.

In order to explain these results, a predominance diagram was calculated for chemical compound speciation using MEDUSA software®. The diagram is shown in Fig. 2.

According to other reports [9,10], uranium carbonate predominates in the presence of dissolved carbon dioxide, which is present in the atmosphere. The following uranium compounds are present at the pH studied of 8.0: $UO_2(CO_3)_2^{2-}$, $UO_2(CO_3)_3^{4-}$ $(UO_2)_2CO_3(OH)_3^-$, $(UO_2)_3(CO_3)_6^{6-}$, $UO_2(OH)_3^-$, $UO_2(OH)_4^{2-}$ and $(UO_2)_2CO_3(OH)_3^-$. These uranium species could interact with the iron species in solution, e.g. iron hydroxides, and all together could co-precipitate onto activated carbon surface, thereby promoting rejection [38].

3.4. *Long-time filtrations*

In order to evidence iron and uranium in membranes, as a support of the hypothesis pointed out above, two long-time filtrations were done to reveal saturation in the membrane surface. The results are shown in Table 5.

Afterwards, the membrane was analyzed by SEM-EDS. The results are presented in Fig. 3.

It can be concluded that iron co-precipitates with uranium, and that both adsorb onto AC, thereby inducing the highest rejection attained for an ultrafiltration process.

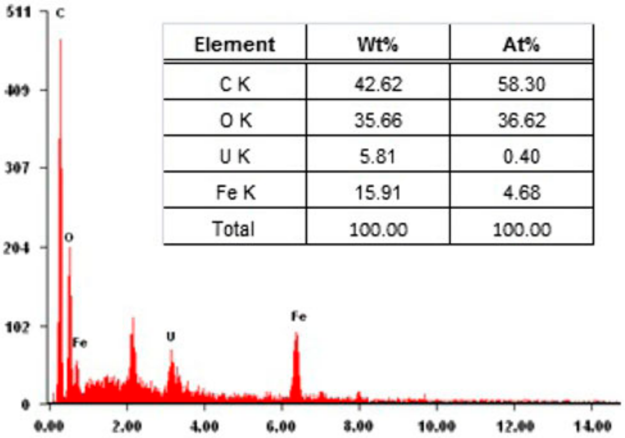

Element	Wt%	At%
C K	42.62	58.30
O K	35.66	36.62
U K	5.81	0.40
Fe K	15.91	4.68
Total	100.00	100.00

Fig. 3. EDS spectrum of CTA–AC membrane section after a long-time filtration. Semi-quantitative data are given in the inset.

4. Conclusion

According to the results presented above, CTA–FeAC membranes are more effective for uranium removal than membranes based on non-doped AC, but with iron in the aqueous solution. Fe6H-based membrane has homogeneous distribution of particles and low roughness, and therefore more iron is available for interacting with uranyl ions. In solutions with uranium and iron, the latter forms a precipitate; therefore, iron interacts in its oxide form. In this case, the solution contains iron in particulate form, and uranium is not efficiently removed. For this reason, the CTA–AC membranes show lower removal efficiencies, compared to CTA–FeAC membranes. In all cases, it was observed that the interaction of iron with uranyl is crucial for proper removal. These membrane processes are promising to remove the concentrations of uranium typically found in drinking water, and those systems where membrane filtration would take place in several stages should achieve better uranium rejection.

Acknowledgements

This research has been partially supported by SEP-CONACYT Project 26040 and Fondos Mixtos

CONACYT—Gobierno del Estado de Chihuahua Projects CHIH-2008-C02-91931 and CHIH-2011-C03-167723. The authors acknowledge the National Nanotechnology Laboratory (NANOTECH) for the use of the scanning electron microscope JSM-5800LV and AFM Nanoscope IVa located in CIMAV, Chihuahua, Mexico. Authors also thank Oscar Solis Canto for AFM measurements.

References

[1] USEPA, Safe Drinking Water Act and Amendments, United States Environmental Protection Agency, Washington, DC, 1996.

[2] SSA, NORMA OFICIAL MEXICANA (OFFICIAL MEXICAN OFFICIAL STANDARD) NOM-127-SSA1-1994, Salud ambiental, agua para uso y consumo humano- Límites permisibles de calidad y tratamientos a que debe someterse el agua para su potabilización, Secretaria de Salud. Volume NOM-127-SSA1-1994, Diario Oficial de la Federación, 2000.

[3] M. Reyes-Cortes, M.E. Montero-Cabrera, M. Rentería-Villalobos, L. Fuentes-Montero, L. Fuentes-Cobas, E.F. Herrera-Peraza, H. Esparza-Ponce, Radioactive mineral samples from the northwest of Chihuahua City, México. Rev. Mex. Fis. S53 (2007) 23–28.

[4] M. Reyes-Cortés, L. Fuentes-Cobas. E. Torres-Moye, H. Esparza-Ponce, M.E. Montero-Cabrera, Uranium minerals from the San Marcos District, Chihuahua, Mexico, Mineral. Petrol. 99 (2010) 121–132.

[5] A. Krestou, A. Xenidis, D. Panias, Mechanism of aqueous uranium (VI) uptake by hydroxyapatite, Miner. Eng. 17 (2004) 373–381.

[6] F.G. Simon, V. Biermann, B. Peplinski, Uranium removal from groundwater using hydroxyapatite, Appl. Geochem. 23 (2008) 2137–2145.

[7] G. Wang, J. Liu, X. Wang, Z. Xie, N. Deng, Adsorption of uranium (VI) from aqueous solution onto cross-linked chitosan, J. Hazard. Mater. 168 (2009) 1053–1058.

[8] A.A. El-Sayed, Kinetics and thermodynamics of adsorption of trace amount of uranium on activated carbon, Radiochim. Acta. 96 (2008) 481–486.

[9] A. Mellah, S. Chegrouche, M. Barkat, The removal of uranium(VI) from aqueous solutions onto activated carbon: Kinetic and thermodynamic investigations, J. Colloid Interface Sci. 296 (2006) 434–441.

[10] C. Kütahyalı, M. Eral, Selective adsorption of uranium from aqueous solutions using activated carbon prepared from charcoal by chemical activation, Sep. Purif. Technol. 40 (2004) 109–114.

[11] A. Schierz, H. Zänker, Aqueous suspensions of carbon nanotubes: Surface oxidation, colloidal stability and uranium sorption, Environ. Pollut. 157 (2009) 1088–1094.

[12] C. Noubactep, A. Schoner, G. Meinrath, Mechanism of uranium removal from the aqueous solution by elemental iron, J. Hazard. Mater. 132 (2006) 202–212.

[13] M. Dickinson, T.B. Scott, The application of zero-valent iron nanoparticles for the remediation of a uranium-contaminated waste effluent, J. Hazard. Mater. 178 (2010) 171–179.

[14] R.A. Crane, M. Dickinson, I.C. Popescu, T.B. Scott, Magnetite and zero-valent iron nanoparticles for the remediation of uranium contaminated environmental water, Water Res. 45 (2011) 2931–2942.

[15] C.-K.D. Hsi, D. Langmuir, Adsorption of uranyl onto ferric oxyhydroxides: Application of the surface complexation site-binding model, Geochim. Cosmochim. Acta. 49 (1985) 1931–1941.

[16] T.D. Waite, J.A. Davis, T.E. Payne, G.A. Waychunas, N. Xu, Uranium(VI) adsorption to ferrihydrite: Application of a surface complexation model, Geochim. Cosmochim. Acta. 58 (1994) 5465–5478.

[17] X. Shuibo, Z. Chun, Z. Xinghuo, Y. Jing, Z. Xiaojian, W. Jingsong, Removal of uranium (VI) from aqueous solution by adsorption of hematite, J. Environ. Radioact. 100 (2009) 162–166.

[18] I.A. Katsoyiannis, Carbonate effects and pH-dependence of uranium sorption onto bacteriogenic iron oxides: Kinetic and equilibrium studies, J. Hazard. Mater. 139 (2007) 31–37.

[19] A. Baeza, A. Salas, F. Legarda, Determining factors in the elimination of uranium and radium from groundwaters during a standard potabilization process, Sci. Total Environ. 406 (2008) 24–34.

[20] T. Gäfvert, C. Ellmark, E. Holm, Removal of radionuclides at a waterworks, J. Environ. Radioact. 63 (2002) 105–115.

[21] C.S. Barton, D.I. Stewart, K. Morris, D.E. Bryant, Performance of three resin-based materials for treating uranium-contaminated groundwater within a PRB, J. Hazard. Mater. 116 (2004) 191–204.

[22] D.H. Phillips, B. Gu, D.B. Watson, C.S. Parmele, Uranium removal from contaminated groundwater by synthetic resins, Water Res. 42 (2008) 260–268.

[23] A.M. St John, R.W. Cattrall, S.D. Kolev. Extraction of uranium (VI) from sulfate solutions using a polymer inclusion membrane containing di-(2-ethylhexyl) phosphoric acid, J. Membr. Sci. 364 (2010) 354–361.

[24] S.D. Kolev, A.M. St John, R.W. Cattrall. Mathematical modeling of the extraction of uranium (VI) into a polymer inclusion membrane composed of PVC and di-(2-ethylhexyl)phosphoric acid, J. Membr. Sci. 425–426 (2013) 169–175.

[25] A.M. St John, R.W. Cattrall, S.D. Kolev. Transport and separation of uranium (VI) by a polymer inclusion membrane based on di-(2-ethylhexyl acid) phosphoric acid, J. Membr. Sci. 409–410 (2012) 242–250.

[26] N. Bayou, O. Arous, M. Amara, H. Kerdjoudj, Elaboration and characterisation of a plasticized cellulose triacetate membrane containing trioctylphosphine oxyde (TOPO): Application to the transport of uranium and molybdenum ions, C.R. Chim. 13 (2010) 1370–1376.

[27] P.K. Mohapatra, D.S. Lakshmi, A. Bhattacharyya, V.K. Manchanda, Evaluation of polymer inclusion membranes containing crown ethers for selective cesium separation from nuclear waste solution, J. Hazard. Mater. 169 (2009) 472–479.

[28] M.I.G.S. Almeida, R.W. Cattrall, S.D. Kolev, Recent trends in extraction and transport of metal ions using polymer inclusion membranes (PIMs), J. Membr. Sci. 415-416 (2012) 9–23.

[29] M.P. Blanco Rodriguez, F Vera Tomé, J.C Lozano, V. Gómez Escobar, Sequential method for the

determination of uranium, thorium and ^{226}Ra by liquid scintillation alpha spectrometry, Appl. Rad. Isot. 52 (2000) 705–710.

[30] J. Leyba, H.S. Vollmar, R.A. Fjeld, T.A. Devol, D.D. Brown, J.R. Cadieux, Evaluation of a direct extraction/liquid scintillation counting technique for the measurement of uranium in water, J. Radioanal. Nucl. Chem. 194 (1995) 337–344.

[31] S.H. Ahmed, C.M. Sharaby, E.M. El Gammal, Uranium extraction from sulfuric acid medium using trioctylamine impregnated activated carbon, Hydrometallurgy. 134–135 (2013) 150–157.

[32] M.L. Hyder, W.C. Perkins, M.C. Thompson, G.A. Burney, E.R. Russell, H.P. Holcomb, L.F. Landon, Processing of irradiated, enriched uranium fuels at the Savannah River Plant, Savannah River Laboratory Report 11527445, 1979.

[33] G.M. Geise, H.B. Park, A.C. Sagle, B.D. Freeman, J.E. McGrath, Water permeability and water/salt selectivity tradeoff in polymers for desalination, J. Membr. Sci. 369 130–138.

[34] O. Raff, R.-D. Wilken, Removal of dissolved uranium by nanofiltration, Desalination 122 (1999) 147–150.

[35] A. Favre-Réguillon, G. Lebuzit, D. Murat, J. Foos, C. Mansour, M. Draye, Selective removal of dissolved uranium in drinking water by nanofiltration, Water Res. 42 (2008) 1160–1166.

[36] A.P. Kryvoruchko, L.Y. Yurlova, I.D. Atamanenko, B.Y. Kornilovich, Ultrafiltration removal of U(VI) from contaminated water, Desalination 162 (2004) 229–236.

[37] P. Huikuri, L. Salonen, O. Raff, Removal of natural radionuclides from drinking water by point of entry reverse osmosis, Desalination 119 (1998) 235–239.

[38] R. Villalobos-Rodríguez, M.E. Montero-Cabrera, H.E. Esparza-Ponce, E.F. Herrera-Peraza, M.L. Ballinas-Casarrubias, Uranium removal from water using cellulose triacetate membranes added with activated carbon, Appl. Radiat. Isot. 70 (2012) 872–881.

[39] G. Muñiz-Chávez, Uso y modificación del carbón activado proveniente de biomasa vegetal para la remoción de arsénico del agua (Use and modification of activated carbon from vegetation biomass for the removal of arsenic from water) (Thesis, M.Sc. Biotechnology), Facultad de Ciencias Químicas, Universidad Autonoma de Chihuahua, Mexico, 2008.

[40] V. Fierro, G. Muñiz, G. Gonzalez-Sánchez, M.L. Ballinas, A. Celzard, Arsenic removal by iron-doped activated carbons prepared by ferric chloride forced hydrolysis, J. Hazard. Mater. 168 (2009) 430–437.

[41] G. Muñiz, V. Fierro, A. Celzard, G. Furdin, G. Gonzalez-Sánchez, M.L. Ballinas, Synthesis, characterization and performance in arsenic removal of iron-doped activated carbons prepared by impregnation with Fe(III) and Fe(II), J. Hazard. Mater. 165 (2009) 893–902.

[42] A. Rueda Ramírez, Métodos de solvatación química para la reducción del tamaño de partícula de carbón activado (Chemical solvation methods for reducing particle size of activated carbon) (Thesis, Bc. Industrial Chemistry), Facultad de Ciencias Químicas, Universidad Autónoma de Chihuahua, Mexico, 2005.

[43] L. Ballinas-Casarrubias, L.P. Terrazas-Bandala, R. Ibarra-Gómez, M.E. Mendoza-Duarte, L. Manjarrez-Nevárez, G. González-Sánchez, Structural and performance variation of activated carbon-polymer films, Polym. Adv. Technol. 17 (2006) 991–999.

[44] I. Horcas, R. Fernández, J.M. Gómez-Rodríguez, J. Colchero, J. Gómez-Herrero, A.M. Baro, WSXM: A software for scanning probe microscopy and a tool for nanotechnology, Rev. Sci. Instrum. 78 (2007) 013705.

[45] M.F. L'Annunciata, M.J. Kessler, Liquid scintillation analysis: Principles and practices, in: M.F. L'Annunciata (Ed.), Handbook of Radioactivity Analysis, second ed., Elsevier, New York, NY, 2003, pp. 397–398.

[46] V. Gómez Escobar, F. Vera Tomé, J.C. Lozano, A. Martín Sánchez. Extractive procedure for uranium determination in water samples by liquid scintillation counting, Appl. Radiat. Isot. 49 (1998) 875–883.

[47] I. Puigdomenech, Hydra/Medusa chemical equilibrium database and plotting software, Inorganic Chemistry, Stockholm, Sweden: KTH Royal Institute of Technology, (2009).

[48] N. Hilal, H. Al-Zoubi, N.A. Darwish, A.W. Mohamma, M. Abu Arabi, A comprehensive review of nanofiltration membranes: Treatment, pretreatment, modelling, and atomic force microscopy, Desalination 170 (2004) 281–308.

[49] J.-H. Jang, B.A. Dempsey, W.D. Burgos, A model-based evaluation of sorptive reactivities of hydrous ferric oxide and hematite for U(VI), Environ. Sci. Technol. 41 (2007) 4305–4310.

[50] I. Grenthe, B. Lagerman, Studies on metal carbonate equilibria. A coulometric study of the uranium (VI)-carbonate system, the composition of the mixed hydroxide carbonate species, Acta Chem. Scand. 45 (1991) 122–128.

[51] C.J. Dodge, A.J. Francis, J.B. Gillow, G.P. Halada, C. Eng, C.R. Clayton, Association of uranium with iron oxides typically formed on corroding steel surfaces, Environ. Sci. Technol. 36 (2002) 3504–3511.

[52] R.A. Crane, M. Dickinson, I.C. Popescu, T.B. Scott, Magnetite and zero-valent iron nanoparticles for the remediation of uranium contaminated environmental water, Water Res. 45 (2011) 2931–2942.

[53] S. Regenspurg, D. Schild, T. Schäfer, F. Huber, M.E. Malmström, Removal of uranium(VI) from the aqueous phase by iron(II) minerals in presence of bicarbonate, Appl. Geochem. 24 (2009) 1617–1625.

Appendix A. Statistical analysis of the results of filtration process

The statistical analysis of the results led to the following equation to predict the removal efficiency RE:

$$\begin{aligned} RE = & 0.2269 - 0.0969 \cdot \%Fe - 0.0502 \cdot pH \\ & + 0.0753 \cdot \%Fe \cdot pH \end{aligned} \tag{A1}$$

Fig. A1 shows the contour response of the uranium removal process using CTA composite membranes loaded with (Fe)AC. The black dots on the contour response correspond to the experimental values of RE.

Fig. A2 shows the response surface of the filtration experiments through CTA composite membranes loaded with (Fe)AC. This curved surface means that both the iron content in the AC and the pH are significant in the removal process, i.e. both parameters contribute to the removal of uranium from water.

From these results, we can conclude that the amount of uranium complexes are maximized at pH 6.0, thereby contributing to increased interaction with the membrane, whereas at pH 7.0 the amount of such species decreases. At pH 8.0, the RE is attributed to the formation of bigger molecules which therefore cannot permeate anymore across the membrane.

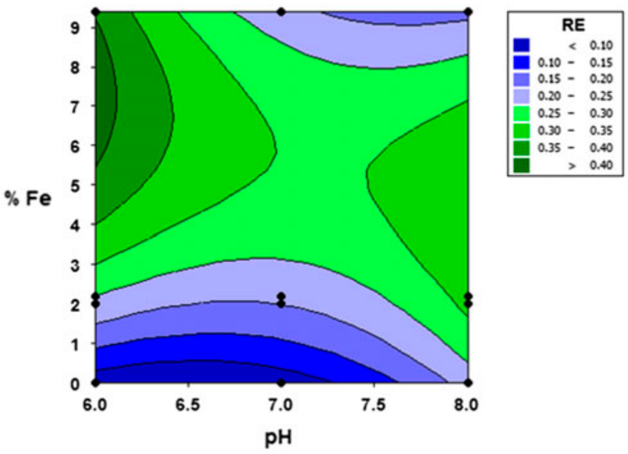

Fig. A1. Response contour of the experimental removal efficiencies.

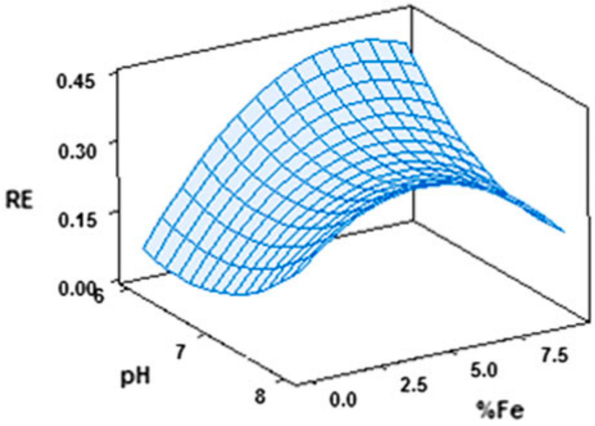

Fig. A2. Response surface of the experimental removal efficiencies.